^{13}C NMR Investigation of a Poly(urethane-urea) System

David T. Okamoto, Stuart L. Cooper, and Thatcher W. Root*

Department of Chemical Engineering, University of Wisconsin—Madison, 1415 Johnson Drive, Madison, Wisconsin 53706

Received June 24, 1991; Revised Manuscript Received September 30, 1991

ABSTRACT: A series of solid-state ^{13}C NMR relaxation experiments was performed on a polyether-poly(urethane-urea) (Biomer) known to possess a microphase-separated morphology. A primary goal was to differentiate between urethane linkages which may be found at the hard segment-soft segment microdomain interface and those dissolved in the soft-segment matrix. $T_1(C)$ and $T_{1\rho}(H)$ measurements can distinguish between the hard-segment and the soft-segment carbons, but not the interfacial region between them. However, differences in the $T_{1\rho}(C)$ behavior for the urea and urethane carbonyl carbons were found, suggesting that the interfacial and dissolved hard segments can be observed by $T_{1\rho}(C)$ but not by $T_{1\rho}(H)$ or $T_1(C)$. Cross-polarization dipolar-dephasing experiments, in conjunction with $T_1(C)$ analysis, indicate that approximately 50% of the hard-segment rings in the sample are able to move as free rotors, without significant hindrance to motion.

I. Introduction

Segmented polyurethane block copolymer systems have been studied by a large number of research groups interested in learning more about both the surface and bulk properties of these compounds. One polymer of significant interest is Biomer, which has been reported to be a segmented polyurethane system primarily based on 4,4'-methylenebis(*p*-phenyl isocyanate) (MDI) hard segments, poly(tetramethylene oxide) (PTMO) soft segments, and an ethylenediamine (ED) chain extender.[1-6] Biomer has been used for blood-contacting applications in the biomedical field because of its biological compatibility and superior physical and mechanical properties. Because of these uses, many studies have focused on either identifying the chemical composition and additives that make up Biomer or determining the surface characteristics of this polyurethane system.

Our primary interest in examining this polymer is to characterize its bulk morphology, utilizing solid-state ^{13}C nuclear magnetic resonance (NMR) to probe different locations within the block copolymer system. Although several polyurethane studies involving ^1H NMR and T_2 deconvolution of the free induction decay have appeared,[7-12] there has been a relative dearth of work utilizing solid-state ^{13}C NMR to characterize polyurethanes.[13-16]

Of particular interest to us in this system is the polyurethane chemistry, which provides for urea linkages between hard-segment units and urethane linkages between hard segments and soft segments. The hard and soft segments are incompatible and form a microphase-separated domain morphology. This chemistry should provide a system where the urea linkages exist primarily inside hard domains, while the urethane linkages are forced to the interfacial region between the hard and soft domains. In addition, hard segments may be encountered which are incapable of phase separation and which will be dissolved within the soft-segment matrix. Thus, we can envision two different types of urethane linkages: those that are part of the hard domains and those that belong to the dissolved hard segments.

Ideally, the different carbon environments (corresponding to the different microphases) would yield different chemical shifts and separate peaks, which could be analyzed easily. This type of behavior has been seen for some homopolymers, such as polyethylene and poly(tetramethylene oxide). Polyethylene exhibits separate peaks at 31.0, 31.3, and 33 ppm, corresponding to the amorphous, interfacial, and crystalline phases, respectively.[17] PTMO with a number-average molecular weight of 67 000 shows peaks at 70.9, 72.0, and 72.9 ppm, corresponding to the amorphous, interfacial, and crystalline regions, respectively.[18] Since none of the carbons in the block copolymer sample appear to exhibit this type of chemical shift dispersion, one must rely on differences in spin relaxation behavior, where they happen to exist. In some cases, differences in mobility and local environment will not provide significant differences in relaxation behavior. One goal of this work was to determine which relaxation studies would be most useful for this class of polymers exhibiting microphase separation.

II. Experimental Section

The solution-grade Biomer sample was taken from a 30% solid solution in *N,N*-dimethylacetamide as received from Ethicon, Inc. (lot BNB 001). The solvent was removed by drying the solution first in a convection oven and then in a vacuum oven at 50 °C for several days. The absence of sharp resonances in the methyl region of the ^{13}C spectrum confirms that no residual solvent was present in the solid sample.

The solids NMR experiments were performed at room temperature on a Chemagnetics CMC-300A FTNMR spectrometer, operating at 75.3 MHz for ^{13}C. Standard phase cycling and quadrature detection were employed. To minimize the effects of long-term drift, the NMR relaxation experiments were block-averaged, ranging from 32 to 64 acquisitions per block. Ten to twenty data subsets were summed and processed on a MicroVAX II computer. Tetramethylsilane (TMS) was used as a frequency reference for the carbon spectra. The Hartmann-Hahn match was set on hexamethylbenzene prior to each sample run.

Magic-angle spinning (MAS) and high-power proton decoupling were employed, with 7.5-mm zirconia rotor spinning speeds on the order of 5.4 kHz. Care was taken to avoid overlapping the first sideband of the soft-segment ether peak with the aromatic or carbonyl carbon shift range. The recycle delay was 5 s and τ_{90} was 5.5 μs for the cross-polarization (CP) spectra, corresponding to a B_1 of 45 kHz. The contact time was varied for the T_{CH} measurements and was set at 1 ms for the $T_{1\rho}(C)$ experiments, with carbon spin-locking pulses[19] ranging from 0 μs to 20 ms. Spin-lattice relaxation data were obtained using a saturation-recovery sequence with gated decoupling. The radiofrequency (rf) field strengths used in the direct-observation experiments were the same as those employed in the CP runs. To obtain integrated peak intensities, the spectra were fit to families of

* To whom correspondence should be addressed.

0024-9297/92/2225-1068$03.00/0

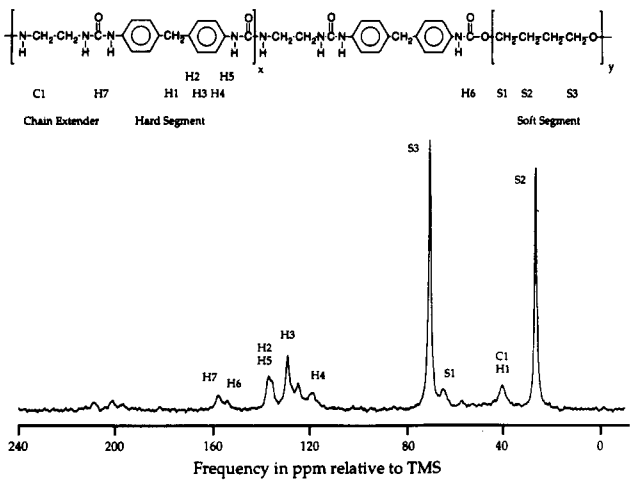

Figure 1. Poly(urethane–urea) chemistry for the system of interest. The system is a 2/1/1 molar ratio of MDI/ED/PTMO, with a soft-segment average molecular weight of 1800.[1,2] The spectrum results from a CPMAS experiment with a contact time of 1 ms.

Table I
Observed ^{13}C Chemical Shifts and NMR Peak Assignments

carbon (label)	chem shift, ppm
PTMO CH_2 adjacent to urethane (S1)	65
PTMO internal CH_2 (S2)	27
PTMO external CH_2 (S3)	71
MDI CH_2 (H1)	41
MDI quaternary ring (H2/H5)	136
MDI protonated ring (H3)	129
MDI protonated ring (H4)	119
MDI urethane carbonyl (H6)	154
MDI urea carbonyl (H7)	158
ED CH_2 (C1)	41

Lorentzian peaks using a nonlinear least-squares routine on a MicroVAX II computer. Relaxation times were then obtained for each resolved carbon peak using the general curve fit provided in KALEIDAGRAPH 2.1.1 for the Macintosh.

III. Results and Discussion

Peak Assignments. The poly(urethane–urea) chemistry for this system along with a CP spectrum is shown in Figure 1, with the carbons labeled according to their source component. That is, the C prefix denotes the chain extender, the H prefix the hard segment, and the S prefix the soft segment. The observed ^{13}C chemical shifts are presented in Table I. These assignments correspond with published values.[14,20-23]

The two peaks observed in the carbonyl region at 154 and 158 ppm are assigned to the urethane (H6) and urea (H7) carbons, respectively. The urethane moiety is located at the soft segment–hard segment boundary and so must either reside in the interfacial region between the hard and soft phases or exist as part of hard segments dissolved in the soft phase. The urea linkage arises from the reaction of the diamine chain extender with the aromatic diisocyanate and so should only reside within the hard domains. On the basis of this model of the morphology, one would expect the urethane carbonyls to exhibit greater mobility compared to the urea carbonyls. This issue is addressed in a later section.

The aliphatic region is dominated by the two soft-segment carbon peaks at 27 and 71 ppm arising from the PTMO soft segment. The smaller peak at 64 ppm is associated with soft-segment carbons that are adjacent to a urethane linkage (S1), while the peak at 71 ppm is assigned to those soft-segment carbons that are adjacent to oxygen (S3). The small peak at 41 ppm is attributed to both the MDI methylene carbon and the ethylenediamine chain extender.[22]

There are five different primary peaks that can be assigned to aromatic carbons ranging from 115 to 140 ppm. The doublet at 136 ppm is due to the quaternary MDI ring carbons (H2, H5), and the peaks at 119 and 129 ppm are due to the protonated aromatic MDI carbons (H3, H4). These assignments are consistent with ^{13}C solution-state spectra.[23] The peak at 125 ppm is not yet assigned; however, if the sum intensity of these five aromatic region peaks is compared to the intensity of the soft-segment methylene peaks in fully-relaxed direct-observation spectra, the resulting ratio is comparable to the value predicted from the polymer stoichiometry.[1,5] This peak at 125 ppm could arise from conformational differences that occur in the solid state. The results from the CP dipolar-dephasing experiments discussed later in this paper support this possibility. Conformationally-induced chemical shifts of 6 ppm between solution- and solid-state NMR spectra have been reported.[24]

Stoichiometry. An estimate of the average soft-segment molecular weight was obtained by performing a least-squares fit to the intensities of the S1, S2, and S3 peaks. Nominally, the average number of repeat units per soft segment could be determined through an end-group calculation by taking the ratio of the fully-relaxed intensities of the S2 peak to the S1 peak. However, the soft-segment molecular weight calculated through this method is extremely sensitive to the S1 peak intensity, which is a relatively weak signal. We used a two-parameter model to find the average number of repeat units in a soft-segment chain and the signal intensity corresponding to a pair of carbons. On the basis of this model, we find an average soft-segment molecular weight of 1300, which is substantially lower than the literature value of 1800. The primary source of error in this calculation probably results from the measurement of the S1 peak intensity, since this peak overlaps with the first set of spinning sidebands from the aromatic carbons. This overlap makes it difficult to determine precisely the baseline in this region.

Methyl Groups as Indicators of Additives. Work by other groups[2,4,5] has identified possible additives, which could appear in carbon NMR spectra. In particular, we were concerned with two components, poly[(diisopropylamino)ethyl methacrylate-*co*-decyl methacrylate] (DIPAM) and 4,4′-butylidenebis(6-*tert*-butyl-*m*-cresol) (Santowhite). The presence of either of these two components in any large amounts should produce NMR signals in the methyl regions, below the 26 ppm soft-segment internal methylene peak. These methyl peaks are the strongest indicator of additives of this system, since nominally there should be no methyl groups in the MDI/ED/PTMO system. The absence of any major peaks in the methyl regions of the spectra indicates that the concentrations of these additives in this sample are low. On the basis of the chemistry of DIPAM, any signal from the acrylate carbonyl will be one-fourth that of the methyl peak from the isopropyl carbons. Therefore, the DIPAM acrylate carbonyl will not complicate the spectra in the important carbonyl shift region from 150 to 160 ppm.

Contact Time and Proton Relaxation Measurements. The T_{CH} and $T_{1\rho}$(H) measurements were obtained by performing CP experiments with variable contact time pulses ranging from 200 μs to 20 ms with a recycle rate of 5 s. Proton T_1 values are typically short (<1 s) and were not studied here. The following form was used to fit the

Table II
T_{CH} and $T_{1\rho}$(H) As Determined from Variable Contact Time Experiments

carbon label	chem shift, ppm	T_{CH}, ms	$T_{1\rho}$(H), ms
S1	65	0.13	3.2
S2	27	1.6	24.1
S3	71	0.75	17.1
H2/H5	136	0.34	6.7
H3	129	0.12	5.2
H4	125	0.11	5.5
H4	119	0.085	4.3
H6	154	0.23	9.0
H7	158	0.39	9.3
H1/C1	41	0.057	4.6

CP peak intensity curves:

$$M(t) = M_1 \exp\left(\frac{-t}{T_{1\rho}(\mathrm{H})}\right)\left(1 - \exp\left(\frac{-t}{T_{CH}}\right)\right) \quad (1)$$

where $M(t)$ is the peak intensity as a function of contact time t; M_1, the normalization constant; $T_{1\rho}$(H), the proton spin–lattice relaxation time in the rotating frame; and T_{CH}, the cross-polarization time constant. The results of the contact time measurements are presented in Table II. From the data, it is possible to identify some qualitative distinctions between the hard and soft segments in terms of their cross-polarization dynamics.

The soft-segment peaks at 27 and 71 ppm exhibit T_{CH} values on the order of 1 ms and $T_{1\rho}$(H) values on the order of 20 ms. The maximum cross-polarization for the soft segment is attained at 4-ms contact time. This slower growth in spin magnetization relative to the hard-segment carbon cross-polarization is consistent with the higher mobility of the soft-phase carbons. The rapid motion of the soft-segment carbons makes the cross-polarization mechanism less efficient than for the hard-segment carbons, even though the soft-segment carbons each have two directly-bonded protons. By employing a relatively short cross-polarization contact time of 1 ms in most of our spectra, for CP experiments we are preferentially observing signal from the hard-segment carbons, which are present at lower concentrations.

The hard-segment carbons exhibit T_{CH} values ranging from 60 to 390 μs and $T_{1\rho}$(H) values ranging from 4 to 9 ms. The maximum cross-polarization signal intensities for the hard-segment carbons occur near 1 ms of contact time. The urea and urethane $T_{1\rho}$(H) are also shorter than the soft segment $T_{1\rho}$(H), being on the order of 9 ms. All of the hard-segment contact time data could be fit adequately by single-component $T_{1\rho}$(H) times. In no case did the data warrant multiple-component $T_{1\rho}$(H) decomposition, even though two-component $T_{1\rho}$(C) behavior was observed for the same peaks.

The fact that the carbon peaks from the two phases possess different $T_{1\rho}$(H) values suggest the possibility of performing proton spin diffusion experiments in the future. It is clear that there are distinct proton spin reservoirs coupled to the different carbons. If proton spin diffusion were extremely rapid, then we would expect a single $T_{1\rho}$(H) for all the carbons, independent of their location on the polymer chain, and this is definitely not occurring.

Carbon Relaxation Measurements. T_1(C) Determinations. ^{13}C spin–lattice relaxation data obtained from saturation–recovery experiments are presented in Table III. The relaxation plots were fit using a two-component model as shown below:

Table III
T_1(C) Relaxation Times and Relative Fractions

carbon label	chem shift, ppm	fast component %	fast component T_1, s	slow component %	slow component T_1, s
S1	65	94	4.62	6	32.4
S2	27	98	0.81	2	26.3
S3	71	98	0.76	2	30.4
H2/H5	136	53	0.80	47	48.6
H3	129	77	0.14	23	17.6
H4	125	53	0.009	47	49.3
H4	119	85	0.07	15	13.6
H6	154	100	4.30		
H7	158	5	0.010	95	145
H1/C1	41	45	0.17	55	13.2

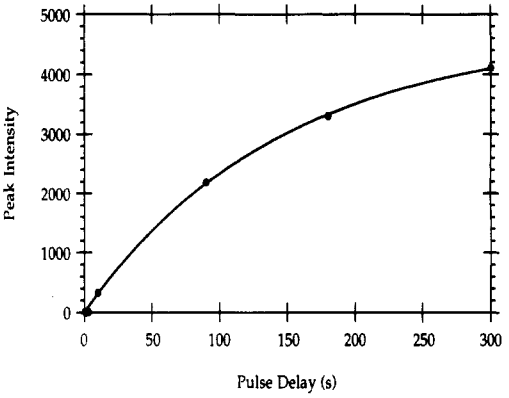

Figure 2. ^{13}C T_1 relaxation plot for the H7 urea carbonyl. The solid line is a nonlinear least-squares fit to the data corresponding to the results in Table III.

$$M(t) = M_A\left(1 - \exp\left(\frac{-t}{T_{1A}}\right)\right) + M_B\left(1 - \exp\left(\frac{-t}{T_{1B}}\right)\right) \quad (2)$$

where M_A and M_B are the equilibrium magnetizations and T_{1A} and T_{1B} are the carbon spin–lattice relaxation time constants for components A and B.

The data indicate that almost all of the soft-segment methylene carbons relax rapidly, on the order of 0.8 s. There is a very small fraction of the S2 and S3 carbons that relaxes much slower, with the T_1(C) closer to that of the hard segment. The S1 carbon, on the other hand, relaxes at a rate that is intermediate between the hard and soft segments and of the same magnitude as the H6 urethane carbonyl carbon. This suggests that both the S1 and H6 carbons have substantial spectral density of motion in the megahertz regime or are sufficiently close to couple to a rapidly-relaxing spin system. It should be noted that a two-component fit to the H6 relaxation curve yielded two components with identical relaxation times, so that a single component sufficed to describe the relaxation behavior. Therefore, we cannot differentiate between the interfacial and dissolved H6 carbons using T_1(C) as a discriminator.

The relaxation curve for the H7 urea carbon is shown in Figure 2. This species has a relatively long T_1, on the order of 145 s. In comparison with the T_1 values for the other hard-segment carbons, this value is rather large. It appears that having two directly-bonded quadrupolar nitrogen nuclei does not provide the urea carbon with an effective mechanism for relaxation. Of the carbons lacking directly-bonded protons, the H7 urea carbon has the longest T_1: comparison with the T_1 of the H2/H5 quaternary ring carbons indicates that part of the weak relaxation may be due to the presence of fewer protons at a distance of two bonds. However, the T_1 for the H6 urethane carbon, which has only one proton at a distance

Table IV
$T_{1\rho}$(C) Relaxation Times and Relative Fractions

carbon label	chem shift, ppm	fast component		slow component	
		%	$T_{1\rho}$, ms	%	$T_{1\rho}$, ms
S1	65	55	3.2	45	11.5
S2	27	16	0.49	84	13.4
S3	71	17	0.49	83	8.6
H2/H5	136	14	0.45	86	21.5
H3	129	16	0.12	83	8.0
H4	125	29	0.13	71	10.5
H4	119	49	1.1	51	9.7
H6	154	27	0.09	73	20.9
H7	158			100	25.1
H1/C1	41	29	0.14	71	4.7

of two bonds, is an order of magnitude faster than that for the H2/H5 carbons. Although both mobility and dipolar coupling contribute to the observed T_1, it appears that the urea carbon is rigid and couples weakly with the lattice. This interpretation is consistent with a picture of the urea carbonyl being strongly hydrogen-bonded to other urea hydrogens within the hard domains.

The aromatic hard-segment carbons appear to be more divided in terms of their T_1(C) behavior, with approximately 60% of the ring carbons relaxing rapidly and the remainder with time constants on the order of 40 s. This is in contrast with the soft-segment and the carbonyl carbons, which tended toward single-component relaxation. However, this two-component behavior is consistent with the results of the CP dipolar-dephasing experiment discussed below, in which one population of the H3 and H4 carbons coupled strongly and one population coupled weakly with the available proton reservoir.

$T_{1\rho}$(C) Determinations. $T_{1\rho}$(C) data were obtained by using a variable-length spin-locking ^{13}C pulse following a standard CP sequence to generate the ^{13}C magnetization. The relaxation plots were fit using a two-component model with the following form:

$$M(t) = M_A \exp\left(\frac{-t}{T_{1\rho A}}\right) + M_B \exp\left(\frac{-t}{T_{1\rho B}}\right) \quad (3)$$

The results from the fit are presented in Table IV.

The soft-segment carbons appear to have similar distributions in terms of their $T_{1\rho}$(C) relaxation times. It has been established from the contact time studies that these carbons cross-polarize at a slower rate than the hard-segment carbons and that the CP conditions employed preferentially enhance the hard-segment signal. For this reason, it is difficult to make quantitative statements concerning the soft-segment carbons. However, the rapidly-relaxing component could correspond with soft segments that are adjacent to the hard-segment domains. Rapid $T_{1\rho}$(C) relaxation can occur when there is a substantial degree of motion at the ^{13}C spin-locking pulse field strength. That is, if there is substantial segmental motion near the 45-kHz spin-locking frequency, then those carbon spins will relax quickly.

The most interesting results from the $T_{1\rho}$(C) study involve the urea and urethane carbons. As described earlier, the chemistry of this system is such that the urea moieties are located inside the hard domains, while the urethane linkages can either be at the interface between the hard and soft domains or be due to dissolved hard segments. The $T_{1\rho}$(C) relaxation plot for the H7 carbon is shown in Figure 3. Although there may be a possibility for a very rapidly-relaxing $T_{1\rho}$(C) component in this data set, it appears that the urea carbon relaxation can be described adequately by a single-component decay, with a time constant of 25.1 ms. This is consistent with the

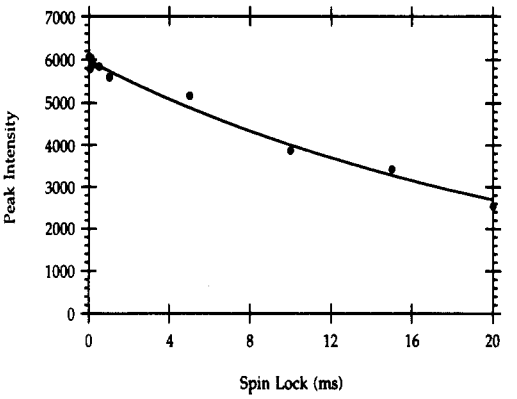

Figure 3. ^{13}C $T_{1\rho}$(C) relaxation plot for the H7 urea carbonyl. The solid line is a nonlinear least-squares fit to the data corresponding to the results in Table IV.

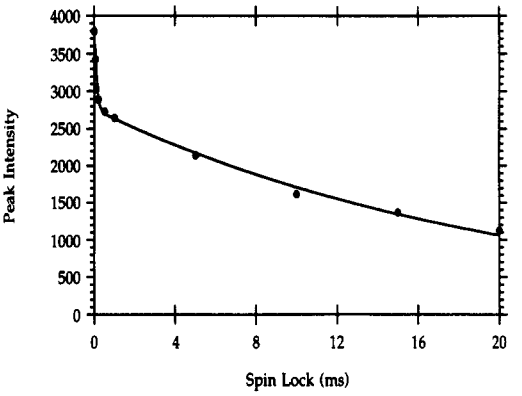

Figure 4. ^{13}C $T_{1\rho}$(C) relaxation plot for the H6 urethane carbonyl. The solid line is a nonlinear least-squares fit to the data corresponding to the results in Table IV.

T_1(C) data, which indicated that the urea carbons were relatively static on the NMR time scale.

In contrast to the urea carbon, the urethane (H6) carbon exhibits distinct two-component relaxation, as shown in Figure 4. Since these urethane moieties only exist where the soft-segment polyol has reacted with the hard-segment isocyanate, these carbons should either be at the domain boundary or dissolved in the soft phase. The longer time constant correlates well with the H7 time constant, suggesting that the slowly-relaxing H6 component is associated with the hard domains and has motional and hydrogen-bonding properties comparable to those of the urea groups. This component corresponds with the urethanes that are at the interface, while the rapidly-relaxing component is associated with the dissolved hard segments. The data indicate that approximately one-fourth of the hard segments are dissolved in the soft phase. Therefore, we can distinguish between dissolved and interfacial carbons using $T_{1\rho}$(C) to discriminate between them.

One difficulty with this interpretation is that the $T_{1\rho}$(C) relaxation data indicate that three-fourths of the urethane carbons have motions similar to the urea carbonyl carbons, but the spin–lattice relaxation data indicate that the ureas are rigid compared to the urethane carbons. However, since we are probing two different motional regimes with the two different carbon experiments, we may be more correct in saying that the urea carbons have very little spectral density of motion at megahertz frequencies compared to the urethane carbons, while the urethane carbons have two distinct populations, both of which have significant spectral density at megahertz frequencies.

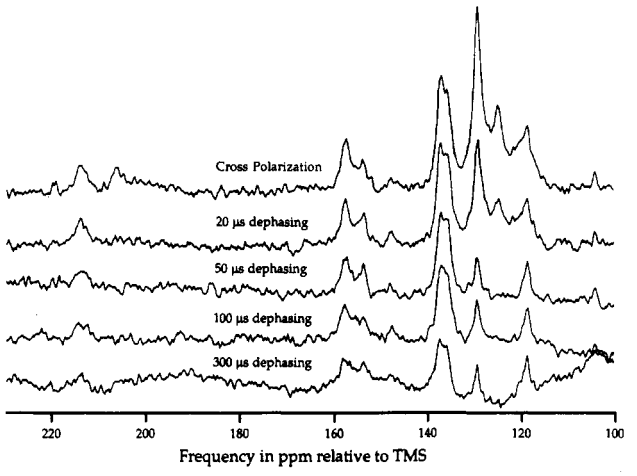

Figure 5. Results of a CP dipolar-dephasing experiment. The small peaks at 104 and 148 ppm are the first spinning sidebands for the S2 and S3 carbons. The peak at 214 ppm corresponds to the first sideband for the H2/H5 carbons.

CP Dipolar-Dephasing Results. CP dipolar-dephasing experiments were performed by allowing the carbon magnetization to dephase in the absence of proton decoupling immediately following a standard CP pulse sequence. The signals were collected with high-power proton-decoupling following this variable delay period. The resulting spectra are shown in Figure 5. Since the proton decoupler is turned off during the dephasing period, those carbons that are strongly coupled with nearby protons will lose their coherence rapidly, on the order of tens of microseconds. If there was a single population of aromatic rings corresponding to the hard phase, then we would expect that the signals from the protonated carbons (H3 and H4) would decay rapidly, while the signals from the quaternary carbons (H2 and H5) would persist for much longer. It is clear, however, that the H3 and H4 signals do not decay as expected.

From this stack plot, we see that the carbons contributing to the peak at 125 ppm are strongly coupled to the proton reservoir. The carbon magnetization at 125 ppm has completely decayed after 50 μs of dipolar dephasing. This peak could arise from a solid-state effect as described earlier, where some of the H4 carbons are relatively static on an NMR time scale and thus experience a slightly different chemical shift than in solution. The rapid decay of the carbon signal at 125 ppm suggests that it is directly bonded to a proton and does not possess the mobility that would serve to average out and weaken the heteronuclear dipolar interaction.

The results of the CP dipolar-dephasing experiment suggest that there are at least two distinct populations of aromatic rings. Although the 119 and 129 ppm protonated ring carbon peaks show rapid decay during the first 50 μs of dipolar dephasing, both peaks still exhibit significant coherence after 300 μs of dephasing. The 129 ppm peak loses 82% of its initial intensity after the first 50 μs but stays approximately constant for the next 250 μs of dephasing time. The persistence of the signal at 119 ppm echos that of the 129 ppm peak. If we sum the fitted intensities for the 125 ppm peak, the 119 ppm peak, and the broad downfield shoulder of the 119 ppm peak and compare this initial value with the 119 ppm peak intensity after 50 μs of dephasing time, we find that this 119 ppm signal is 17% of the initial sum. That is, both slowly-relaxing protonated aromatic carbons signals represent approximately 20% of the initial intensity.

This indicates that there is one population of protonated ring carbons strongly coupled to the proton reservoir and one population that possesses very weak heteronuclear coupling. The population that is coupled strongly is likely to be associated with the glassy hard domains, where the segmental mobility is restricted. On the other hand, the aromatic rings that are part of the dissolved hard segments should have very little restriction and could be acting as free rotors, with very low potential energy barriers for rotation. If there is only free rotation about the H2–H5 axis during the NMR experiment, this would cause an 88% decrease in the coupling strength. If the entire hard segment were capable of isotropic tumbling, then the decrease in the dipolar coupling would be even greater.

On the basis of these motional-averaging arguments, the short T_1(C) component discussed earlier can be associated with the longer dipolar-dephasing time, and the longer T_1(C) component with the rapidly-decaying dipolar-dephasing time. Since the mobile rings have T_1(C) on the order of or shorter than the soft-segment T_1(C), this seems to suggest that these rings are capable of very rapid motion and exist as free rotors in the soft domain. From the T_1(C) section earlier, we found approximately 60% of the aromatic ring carbons exhibited short T_1(C) behavior, while the CP dipolar-dephasing experiments indicated only 20% of the aromatic rings with long dephasing times. Since the dipolar-dephasing experiment utilizes cross-polarization to generate the carbon magnetization, this experiment may discriminate against the highly mobile rings in the same manner that CP is less efficient for the soft-segment carbons. A more detailed study of the dipolar-dephasing behavior would be necessary to produce a precise quantitative breakdown of the ring populations, but the results that we have presented are sufficient to gain a good picture of the polymer morphology.

In addition, approximately 50% of the carbon magnetization at 136 ppm corresponding to the quaternary ring carbons still exists after 300 μs of dipolar-dephasing time. Both the urea and urethane carbonyl carbons still retain coherence after 300 μs of dipolar dephasing. This is not surprising, since these carbons possess no directly-bonded protons.

IV. Summary and Conclusions

Through a series of ^{13}C NMR experiments, it has been possible to develop some insight into the types of motions available to different portions of the poly(urethane–urea) chain. Although the solid-state ^{13}C spectra of this system are complex and no simple peak shifts are observed for the different microphases of the room temperature sample, we can detect differences in the morphology by investigating the appropriate spin relaxation regime.

The magnitude of the urea carbon T_1(C) suggests that these groups are severely restricted in the hard domains and do not possess the mobility that the urethane carbonyls have, since the urethane carbons exhibit a T_1(C) that is 20 times shorter. However, we can only find a single characteristic T_1(C) relaxation time for the urethane carbons, indicating that the two separate populations corresponding to the interfacial and dissolved urethane carbonyls have comparable motional characteristics and spectral density in the megahertz region and cannot be distinguished in this fashion.

The most significant NMR results bearing on the hard-segment distribution between hard domains and dissolved environments are the carbon $T_{1\rho}$ measurements. The contact time experiments show that the urea and urethane carbonyls have similar T_{CH} and $T_{1\rho}$(H) times, and the

urethane carbonyl carbons do not exhibit noticeable differences in their $T_{1\rho}$(H) behavior. The $T_{1\rho}$(C) relaxation curves for the urea and urethanes reveal that the urea carbons are adequately described by a single relaxation time, while the urethane carbons display two-component behavior. The longer $T_{1\rho}$(C) for the urethane is comparable to the $T_{1\rho}$(C) for the urea groups, indicating that this component is associated with the hard domains, and thus this population is the interfacial urethane carbons. The remaining urethanes, with their rapid $T_{1\rho}$(C) relaxation, are assigned to isolated hard-segment moieties dissolved in the soft-segment matrix.

The results of the CP dipolar-dephasing experiment also seem to indicate that a good fraction of the hard-segment units are dissolved in the soft phase, as might be expected from the stoichiometry of the polymer. There is a population which decays rapidly, as expected for rigid domains with consequent strong C–H dipolar coupling, but there is also a component which exhibits very weak coupling even to directly-bonded protons. This is compatible with a population of aromatic rings that are essentially behaving as free rotors, with very low potential energy barriers for rotation.

A major difficulty with studying these types of polymer systems in natural abundance, as would be most generally useful, is that often the most interesting signals are the weakest signals. This requires a relatively large amount of spectrometer time to characterize the sample, and thus it is important to determine which relaxation parameters should be probed to make the most efficient use of available instrument time. In this study of a phase-separated poly(urethane–urea) block copolymer, $T_{1\rho}$(C) is clearly the most useful relaxation experiment for determining hard-segment locations, especially when supplemented with CP dipolar-dephasing experiments.

Acknowledgment. The solid-state NMR spectrometer employed in this work was purchased with the financial support of the Shell Oil Foundation. Support for this research was provided by NSF Grants CBT-8657496 and DMR-8603839, by NIH Grants HL-21001 and HL-24046, and by the Shell Oil Foundation. Acknowledgment is made to Robert Hergenrother for helpful discussions concerning the Biomer sample.

References and Notes

(1) Lelah, M. D.; Lambrecht, L. K.; Young, B. R.; Cooper, S. L. *J. Biomed. Mater. Res.* **1983**, *17*, 1.
(2) Richards, J. M.; McClennen, W. H.; Meuzelaar, H. L. C.; Shockcor, J. P.; Lattimer, R. P. *J. Appl. Polym. Sci.* **1987**, *34*, 1967.
(3) Gogolewski, S. *Colloid Polym. Sci.* **1989**, *267*, 757.
(4) Richards, J. M.; McClennen, W. H.; Meuzelaar, H. L. C. *J. Appl. Polym. Sci.* **1990**, *40*, 1.
(5) Belisle, J.; Maier, S. K.; Tucker, J. A. *J. Biomed. Mater. Res.* **1990**, *24*, 1585.
(6) Chinn, J. A.; Posso, S. E.; Horbett, T. A.; Ratner, B. D. *J. Biomed. Mater. Res.* **1991**, *25*, 535.
(7) Assink, R. A. *J. Polym. Sci., Polym. Phys. Ed.* **1977**, *15*, 59.
(8) Assink, R. A.; Wilkes, G. L. *Polym. Eng. Sci.* **1977**, *17*, 606.
(9) Assink, R. A.; Wilkes, G. L. *J. Appl. Polym. Sci.* **1981**, *26*, 3689.
(10) Assink, R. A. *J. Appl. Polym. Sci.* **1985**, *30*, 2701.
(11) Nierzwicki, W. *J. Appl. Polym. Sci.* **1984**, *29*, 1203.
(12) Nierzwicki, W. *J. Appl. Polym. Sci.* **1987**, *33*, 1241.
(13) Eisenbach, C. D.; Gronski, W. *Makromol. Chem., Rapid Commun.* **1983**, *4*, 707.
(14) Christenson, C. P.; Harthcock, M. A.; Meadows, M. D.; Spell, H. L.; Howard, W. L.; Creswick, M. W.; Guerra, R. E.; Turner, R. B. *J. Polym. Sci., Polym. Phys. Ed.* **1986**, *24*, 1401.
(15) Meadows, M. D.; Christenson, C. P.; Howard, W. L.; Harthcock, M. A.; Guerra, R. E.; Turner, R. B. *Macromolecules* **1990**, *23*, 2440.
(16) Parker, A. A.; Marcinko, J. J.; Shieh, Y. T.; Shields, C.; Hedrick, D. P.; Ritchey, W. M. *Polym. Bull.* **1989**, *21*, 229.
(17) Kitamaru, R.; Horii, F.; Murayama, K. *Macromolecules* **1986**, *19*, 636.
(18) Hirai, A.; Horii, F.; Kitamaru, R.; Fatou, J. G.; Bello, A. *Macromolecules* **1990**, *23*, 2913.
(19) Schaefer, J.; Stejskal, E. O.; Buchdahl, R. *Macromolecules* **1977**, *10*, 384.
(20) Delides, C.; Pethrick, R. A.; Cunliffe, A. V.; Klein, P. G. *Polymer* **1981**, *22*, 1205.
(21) Kricheldorf, H. R. *J. Macromol. Sci., Chem.* **1980**, *A14*, 959.
(22) Kricheldorf, H. R.; Hull, W. E. *Makromol. Chem.* **1981**, *182*, 1177.
(23) Kaji, A.; Murano, M. *Polym. J.* **1990**, *22*, 1065.
(24) VanderHart, D. L.; Earl, W. L.; Garroway, A N. *J. Magn. Reson.* **1981**, *44*, 361.